第 28 卷第 12 期 无 机 化 学 学 报 Vol.28 No.12
2012 年 12 月 CHINESE JOURNAL OF INORGANIC CHEMISTRY 2565-2572

KOH 活化的炭干凝胶及其储氢性能

张静娴[1] 易观贵[1] 刘应亮*,[1] 吴拥建[1] 肖 勇[1] 孙立贤[2]
([1]暨南大学化学系,纳米化学研究所,广州 510632)
([2]中科院大连化学物理研究所,大连 116023)

摘要: 以苯二酚与甲醛为前驱体,赖氨酸作为催化剂,快速合成了有机溶胶。有机溶胶经碳化以及 KOH 进一步活化,获得了具有较高微孔率和较大比表面积的炭干凝胶。研究了多孔炭干凝胶的储氢性能,比较了不同活化程度的炭干凝胶的最大储氢容量与比表面积、微孔体积以及微孔孔径分布的关系。结果表明,KOH 适度活化的炭干凝胶(ACX-5)具有较高的比表面积(2 204 $m^2 \cdot g^{-1}$) 和较大的总孔容积(1.09 $cm^3 \cdot g^{-1}$),在 77 K 和 1.1 MPa 氢压下时其储氢量可达 4.3wt%。

关键词: 炭干凝胶; KOH 活化; 储氢
中图分类号: TQ127.1 **文献标识码**: A **文章编号**: 1001-4861(2012)12-2565-08

KOH-Activated Carbon Xerogels for Hydrogen Storage

ZHANG Jing-Xian[1] YI Guan-Gui[1] LIU Ying-Liang*,[1] WU Yong-Jian[1] XIAO-Yong[1] SUN Li-Xian[2]
([1]*Department of Chemistry and Institute of Nanochemistry, Jinan University, Guangzhou* 510632, *China*)
([2]*Dalian Institute of Chemical Physics, Chinese Academy of Sciences, Dalian, Liaoning* 116023, *China*)

Abstract: Organic xerogel was rapidly prepared via a lysine-catalyzed gelation process with resorcinol and formaldehyde as the precursors. After carbonization and a subsequent activation with KOH, carbon xerogels with high microporosity and high-specific-surface area could be obtained. The hydrogen storage properties of the porous carbon xerogels were studied. The relationship of the maximum hydrogen storage capacity with specific surfacearea, micropore volume and pore size distribution was investigated. The results show that moderately KOH-activated carbon xerogel (ACX-5) with high surface area of 2 204 $m^2 \cdot g^{-1}$ and large total-pore volume of 1.09 $cm^3 \cdot g^{-1}$ exhibits the largest hydrogen storage capacity of 4.3wt% at 77 K and under 1.1 MPa hydrogen pressure.

Key words: carbon xerogels; KOH activation; hydrogen storage

Hydrogen has been recognized as an ideal energy carrier due to its abundant, renewable, burning pollution-free and higher chemical energy than hydrocarbon fuels[1]. However, the storage and transportation of hydrogen in a safe and efficient way is the key challenge in large-scale applications of hydrogen energy. Currently, there are essentially several ways to store hydrogen, including liquefaction, compressed gas, metal hydrides, chemical hydrides, and porous adsorbents. Among them, the adsorption of hydrogen on porous materials is a physical adsorption process, which possesses a number of advantages, such as fast kinetics, weak bonding in gas-solid interaction, high energy efficiency and complete

收稿日期:2011-11-28。收修改稿日期:2012-06-02。
国家-广东联合基金(No.U0734005);中央高校基本科研业务费专项资金(No.21610102);国家自然科学基金(No.21031001);广东省高等学校科技创新重点项目(No.cxzd1014)资助项目。
*通讯联系人。E-mail:tliuyl@jnu.edu.cn; 会员登记号:S060017521P。

reversibility. Porous materials with high specific surface area and large micropore volume can enhance the hydrogen storage capacity on the basis of physisorption[2-4].

On the other hand, carbon xerogels have drawn much attention as effective physisorbents because of the favorable properties such as high specific surface area, microporosity, low mass and good adsorption capacity. It was reported that the excess wt% of hydrogen in carbon xerogels reached 5.3wt% at 77 K under 3 MPa hydrogen pressure[5], which is close to the gravimetric hydrogen storage density target of 6wt% H_2 in 2010 established by the US Department of Energy(DOE). In another study[6], the hydrogen storage properties of two types of carbon aerogels, i.e. KOH catalyzed and uncatalyzed samples showed that a KOH catalyzed carbon aerogel enhanced hydrogen storage capacity, exhibiting a hydrogen uptake of 5.2wt% at 77 K under 3.5 MPa hydrogen pressure. Recently, metal-doped carbon aerogels materials, such as Ni-doped carbon xerogels[7] and Co doped carbon aerogels[8] have been investigated for H_2 storage.

Usually, carbon xerogels are derived from the polycondensation of resorcinol (R) with formaldehyde (F). In a typical process, resorcinol-formaldehyde (RF) aerogels are prepared via a base (Na_2CO_3)-catalyzed gelation of aqueous solutions of resorcinol with formaldehyde, followed by aging and drying from superctitical fluid (SCF) CO_2[9-12]. The major drawback of the base-catalyzed method is the long gelation time, which typically takes a couple of days[5]. Even the time-efficient synthesis[13], a gelation catalyzed by HCl, requires 2 h at room temperature. Moreover, catalysts such as Na_2CO_3 and HCl used to improve gelation times may result in impurities (e.g. Na^+, Cl^-) in the final product.

In this work, we prepared carbon xerogels by a lysine-catalyzed gelation process with resorcinol and formaldehyde as precursors. Compared with the usual base or HCl-catalyzed process, the lysine-catalyzed gelation process is completed within 3 minutes rather than days or hours, leading to a very fast formation of a gel. After carbonization and a subsequent activation with KOH, carbon xerogels with high microporosity and high-specific-surface area could be obtained. The effects of the mass ratio of KOH and carbon xerogel on the surface area and micropore volume were investigated, and the hydrogen storage properties of the porous carbon xerogels were tested.

1 Experimental

1.1 Synthesis of carbon xerogels

The process for preparation of porous carbon xerogels is shown in Fig.1. It involves the polymerization of resorcinol and formaldehyde in the presence of lysine, a thermal treatment and carbonization process to synthesize carbon xerogels, and a subsequent KOH activation process to form porous carbon xerogels. In a typical synthesis, RF gels with a 1:2 molar ratio were prepared by mixing two solutions of resorcinol and formaldehyde at room temperature according to the reference[14]: solution "A" containing 1.5 g of resorcinol and 2.21 g of formaldehyde (37wt%). Solution B contains 0.25 g of *L*-lysine dissolved in 3 mL water. Solution A was quickly decanted into solution B with vigorous stirring to obtain a homogeneous solution. Within 3 minutes, a yellow bulk polymer was prepared. Then the gel was dried at 50 ℃ without any pre-treatment, followed by annealing in N_2 at 800 ℃ for 1 h, with a heating rate of 5 ℃·min^{-1}.

KOH activation was carried out under N_2 flow by heating the physical mixture of KOH and the prepared carbon xerogels. The corresponding product is denoted as ACX-*n* (ACX means activated carbon xerogels and *n* equals to the mass ratio of KOH and carbon xerogels). When the mass ratio of the KOH to carbon xerogel (KOH/C) is set at 2, 3, 4, and 5, accordingly, the activated sample is denoted as ACX-2, ACX-3, ACX-4 and ACX-5, respectively. For comparison, one unactivated sample referred as ACX-0 was also prepared. All samples were annealed in N_2 at 850 ℃ for 1 h, with a heating rate of 1.25 ℃·min^{-1}. After natural cooling, the resultant carbon materials were washed with 3 mol·L^{-1} hydrochloric acid and rinsed with hot double-distilled water to remove potassium residues, and dried overnight.

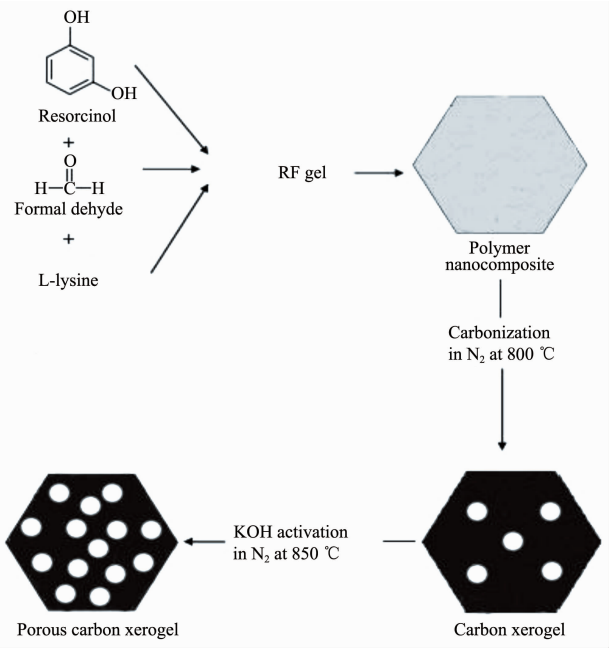

Fig.1　Scheme for lysine-catalyzed synthesis of porous carbon xerogel sample

1.2　Characterization

The morphologies were observed by a Philips SEM-XL30S scanning electron microscope (SEM). The pore characteristics such as specific surface area, pore size distribution and pore volume were estimated by analyzing N_2 adsorption isotherm profiles at 77 K, which were obtained using Micromertics TriStar 3000 Analyzer and Micromeritics ASAP 2020 system. The specific surface area S_{BET} was calculated on the basis of the Brunauere Emmette Teller (BET) model[15]. The meso- and micropore sizes of samples were analyzed by the Barrett-Joyner-Halenda (BJH) and HK methods, respectively. The total pore volume was calculated at a relative pressure of about 0.995. The mesopore volume was obtained by subtracting micropore volume from the total pore volume. Finally, H_2 adsorption was measured by volumetric method under the pressure range of 0~1 bar at 77 K by using the Micromeritics ASAP 2020 system.

1.3　Hydrogen Storage Measurement

Hydrogen adsorption was measured with a Sieverts apparatus at 298 K (room temperature) and 77 K (liquid N_2 temperature) over the pressure range of 0~1.1 MPa. The purity of hydrogen was 99.9999% and the mass of each measured sample was more than 0.5 g. Before measurement, all samples were degassed in vacuum at 200 ℃ for at least 4 h. The apparatus was previously tested by using a typical standard material, $LaNi_5$, to prove the system to be leak-free and accurate.

2　Results and discussion

2.1　Characterization of the samples

The surface morphologies of the samples ACX-5 and ACX-0 are shown in Fig.2. Clearly, well-developed porous structures are formed after KOH activation, as shown in Fig.2a. The other KOH activated samples, from ACX-2 to ACX-4, show similar surface morphologies with sample ACX-5. But the morphology of sample ACX-0 is very different from KOH activated samples, which does not show any porous architecture, see Fig.2b.

It is generally acknowledged that during KOH activation, several reactions take place[16-18](Eqs.(**1**)-(**4**)):

$$6KOH+2C\rightarrow 2K+3H_2+2K_2CO_3 \quad (\mathbf{1})$$

$$K_2CO_3\rightarrow K_2O+CO_2 \quad (\mathbf{2})$$

$$K_2CO_3+2C\rightarrow 2K+3CO \quad (\mathbf{3})$$

$$K_2O+C\rightarrow 2K+CO \quad (\mathbf{4})$$

Whilst potassium reduction to the elemental state is spontaneous above 570 ℃(Eq.(**1**)), higher temperatures (*i.e.* T >700 ℃) are required to decompose

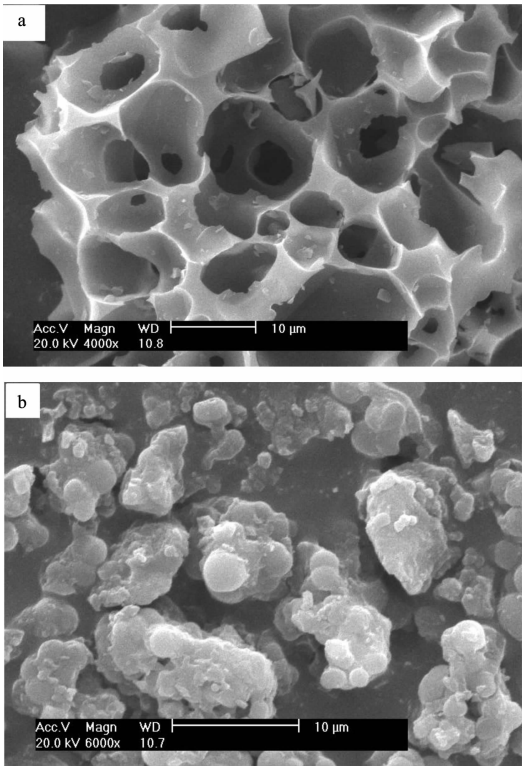

Fig.2 SEM images of ACX-5 (a) and ACX-0 (b) samples

potassium carbonate and oxide into metallic potassium (T_{ev}=759 ℃) and carbon oxides (Eqs.(**2**)~(**4**)).

Eq.(**2**) is particularly worthy of note as it involves formation of CO_2, which can further react with the carbon matrix, as in physical activation[17].

All these processes contribute to the formation of pores in the carbon matrix.

The FTIR spectra of all samples are shown in Fig. 3. It is clear that there are functional groups such as O-H, C-H, C =O and C-O in sample ACX-0. But the functional groups, C =O and C-O, decrease to some extent after KOH-activation, as shown on ACX-2, 3, 4, 5. It is believed that the C-O bonds break during the activation process, which weakens the force between carbon molecules and also promotes the formation of pore structure.

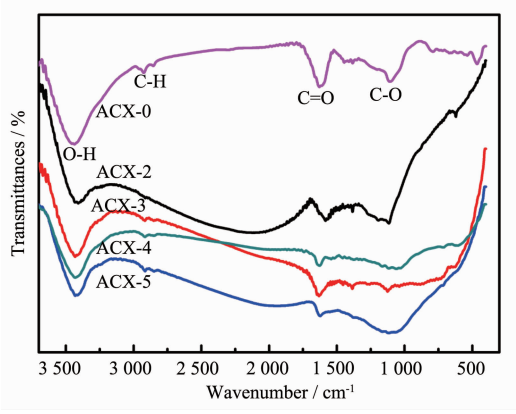

Fig.3 FTIR spectra of carbon xerogel samples

2.2 Adsorption and desorption isotherms

To study the effect of the mass ratio of KOH/C on the nanoporous architecture of the obtained materials, nitrogen adsorption and desorption isotherms were measured at 77 K. As shown in Fig.4, the nitrogen sorption-desorption isotherms conform to type I of the isotherm[19]. At first, the adsorption increases gradually with the increasing of the pressure, then it remains stable resulting in a platform on the isotherm. The isotherm indicates that the adsorbent has microporous structure.

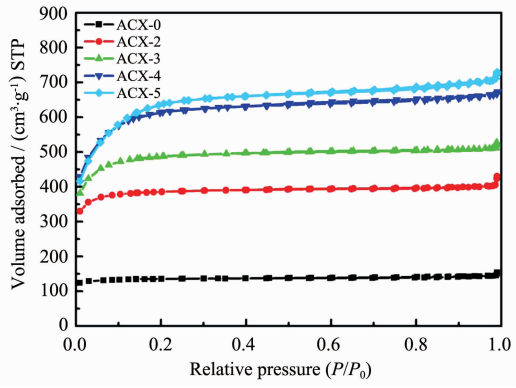

Fig.4 N_2 adsorption/desorption isotherms of carbon xerogel samples at 77 K

Previous studies have shown that microporous adsorption is not surface coverage, but the volume filling of micropores[20]. As the diameter of micropore is no more than a few molecules, the superposition of the potential field related to the hole wall enhances the interaction energy between the solid surface and the gas molecules, thereby enhances the absorption at first stage. So the gas molecules could be absorbed in micropore at a low pressure. When the pores are filled full, there is only a small increase in adsorption capacity even if the pressure increases. Therefore, there is a platform on the curve. In addition, the adsorption and desorption are reversible process, and the desorption and adsorption isotherm overlap with no hysteresis.

In this experiment, the isotherms of all samples,

from ACX-2 to ACX-5, are Type I isotherms. So, it could be concluded that the adsorbents, KOH-activated carbon xerogels, are microporous solids.

Carbon xerogels are typical mesoporous materials. In this study, the mesoporous carbon materials with high surface area are prepared if the polymer is activated with KOH directly. If the polymer is annealed in N_2 for some time before activation with KOH, microporous carbon materials are obtained because the nitrogen pyrolysis process promotes the formation of micropore. A preliminary view is that the carbon materials are condensed during the pyrolysis process, which contributes to the formation of micropore after a subsequent activation with KOH.

Table 1 gives the values of both microporous volumes and areas. It shows that the S_{BET} of the KOH-activated samples is distributed in the range from 1 295 to 2 204 $m^2 \cdot g^{-1}$ and sample ACX-5 achieves a high surface area of 2 204 $m^2 \cdot g^{-1}$. The relationship between the specific surface area and the mass ratio of KOH/C is shown in Fig.5a. It shows that the specific surface area increases with the increasing of the mass ratio of KOH/C.

Table 1 also shows that all activated samples exhibit higher total volumes and micropore volumes than the unactivated carbon xerogel. The pore-structure parameters of samples prove that all KOH-activated carbon xerogels are highly microporous materials.

Table 1　Surface area and pore-structure parameters of the samples

Sample	m_{KOH} / m_{carbon}	S_{BET}[a] / ($m^2 \cdot g^{-1}$)	S_{micro}[b] / ($m^2 \cdot g^{-1}$)	V_t[c] / ($cm^3 \cdot g^{-1}$)	V_{micro}[d] / ($cm^3 \cdot g^{-1}$)	V_{meso}[e] / ($cm^3 \cdot g^{-1}$)	V_{micro} / V_{total} / %	D_{BJH}[f] / nm
ACX-0	0:1	451	406	0.22	0.19	0.03	86.4	1.97
ACX-2	2:1	1 295	1 138	0.62	0.53	0.09	85.5	1.92
ACX-3	3:1	1 644	1 367	0.79	0.63	0.16	79.7	1.92
ACX-4	4:1	2 084	1 437	1.02	0.66	0.36	64.7	1.96
ACX-5	5:1	2 204	1 276	1.09	0.60	0.49	55.0	1.98

[a] The specific surface area (S_{BET}) is calculated by the Brunauer-Emmett-Teller (BET) method

[b] S_{micro} represents the micropore area

[c] V_t denotes the total-pore volume

[d] V_{micro} represents the micropore volume

[e] V_{meso} stands for the Barrett Mesopore volume obtained by subtracting V_{micro} from V_t

[f] D_{BJH} stands for the Barrett-Joyner-Halenda (BJH) desorption average pore width

As shown in Fig.5b, the total volume is proportional to the mass ratio of KOH/C and gradually increases from 0.22 $cm^3 \cdot g^{-1}$ for ACX-0 to 1.09 $cm^3 \cdot g^{-1}$ for ACX-5. Moreover, an increase in KOH/C value increases the microporosity correspondingly. When the mass ratio of KOH/C is set as 4, the micropore volume reaches a maximum value of 0.66 $cm^3 \cdot g^{-1}$. But a higher KOH content brings a decrease of micropore volume.

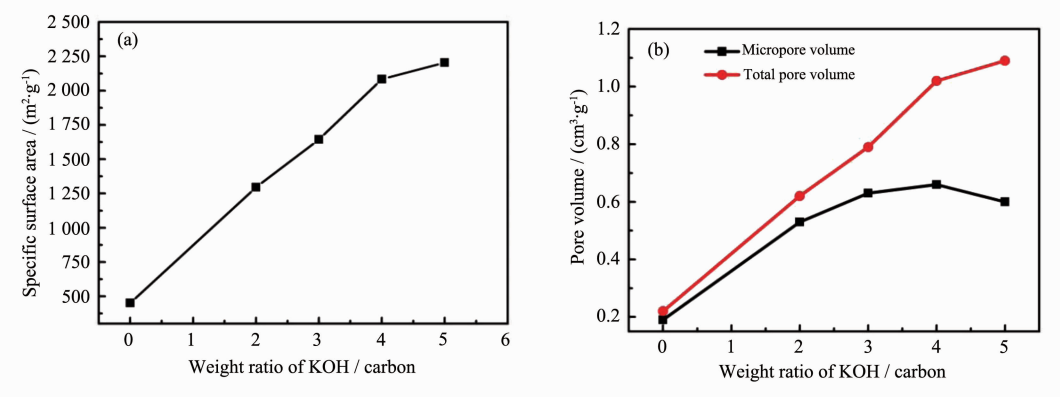

Fig.5　Relationships between specific surface area (a), pore volume (b) and the weight ratio of KOH/carbon for the samples

When the mass ratio of KOH/C is increased to 5, the micropore volume decreases to 0.60 $cm^3 \cdot g^{-1}$ and small mesopores developes as the result of the widening of the pre-existing micropores[21].

2.3 Hydrogen storage capacity

The hydrogen storage capacities of the KOH-activated carbon xerogels have been investigated at 298 K. As shown in Fig.6, the hydrogen storage capacities increase monotonically for all the samples along with elevation of the applied pressure. Among the materials studied in present work, sample ACX-5 with the highest activation degree shows the largest hydrogen storage capacity of 0.31wt% under 1.1 MPa hydrogen pressure, which is two times of the unactivated sample ACX-0 (0.15wt%).

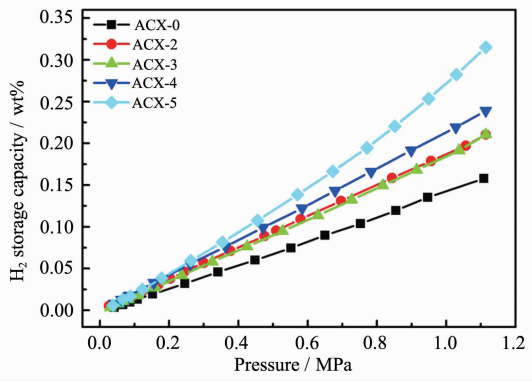

Fig.6 Change of hydrogen storage capacities of the samples with equilibrium hydrogen pressure at 298 K

The hydrogen uptake, measured at 77 K over the hydrogen pressure range 0~1.1 MPa , is shown in Fig.7. Clearly, the hydrogen storage capacities of the carbon xerogels are markedly improved after the activation. It is notable that the maximum hydrogen uptakes of ACX-5 is 4.3% under 1.1 MPa hydrogen pressure, which is higher than that of carbon materials with microporous structures fabricated from coffee beans wastes through KOH activation, which is 4.0wt% under 4 MPa hydrogen pressure at 77 K[22].

Comparing Fig.6 with Fig.7, it can be conclude that the hydrogen storage capacities of all samples at 77 K are larger than those at 298 K. The result is consistent with those obtained from other studies[21,23].

Generally, it is expected that materials with high

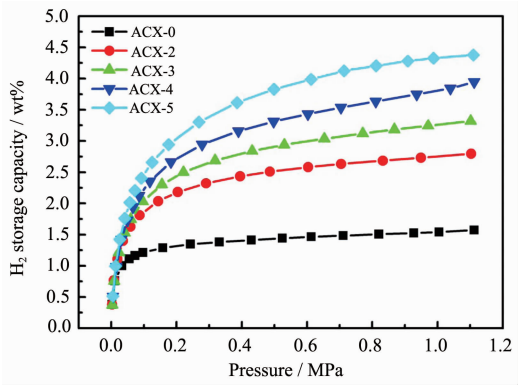

Fig.7 H_2 uptake curves of all samples at 77 K over the hydrogen pressure range 0.0~1.1 MPa

surface area and high total pore volume certainly provide more accessible adsorbing sites, therefore, have excellent hydrogen storage properties. In the present work, it shows a better linear relationship between the hydrogen adsorption capacity and specific surface area S_{BET} at both 298 K and 77 K, as shown in Fig.8a.

Fig.8b shows the relationship between the maximum hydrogen adsorption capacity and micropore volume at 298 K and 77 K, indicating that the hydrogen

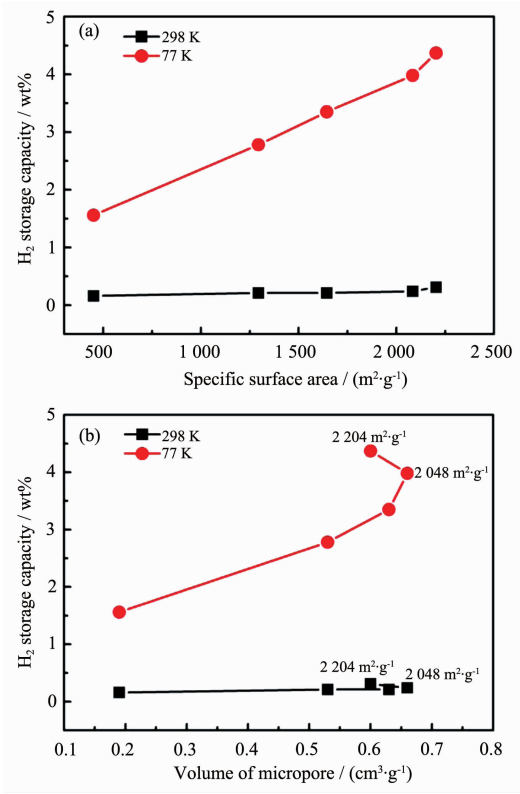

Fig.8 Relationships between the hydrogen storage capacities and specific surface area (a), and micropore volume (b) of the samples

storage ability of the carbon xerogels is essentially affected by the micropore volume.

As discussed above, the microporous adsorption is not surface coverage, but the volume filling of micropores. The hydrogen adsorption process in carbon porous materials at moderate temperature is due to physical adsorption based on van der Waals forces between adsorbent and adsorbate. So, with the micropore volume of the samples increases, the developed micropores provide the carbon xerogels a larger adsorption potential and a stronger interaction with the hydrogen molecules as a result of the maximum hydrogen adsorption capacity increasing from ACX-0 to ACX-4.

It should be noted that sample ACX-5 has a smaller micropore volume than ACX-4 (i.e., 0.60 $cm^3 \cdot g^{-1}$ and 0.66 $cm^3 \cdot g^{-1}$, respectively) but the former has a high hydrogen adsorption capacity. The BET surface area plays an important role in hydrogen adsorption capacity and hydrogen storage capacity is proportional to BET surface area generally, just as shown in Fig.8a. The highest surface area of 2 204 $m^2 \cdot g^{-1}$ and, therefore, the highest H_2 adsorption capacity corresponds to sample ACX-5. In addition, there are other characteristics (*i.e.*, micropore size distribution) that have a great influence on H_2 adsorption capacity [24]. Fig.9 presents pore size distributions for KOH-activated samples. As can be seen from Fig.9, samples ACX-2, ACX-3 and ACX-4 present similar micropore size distributions, but sample ACX-5 has a narrower micropore size distribution than the other. Most of the studies have accepted that highly microporous materials with a narrow micropore size distribution centered at a pore size of around 0.7 nm are the most suitable for H_2 hydrogen storage [24-29]. So, it can concluded that the narrow microporosity also notably influence the H_2 adsorption capacity of sample ACX-5.

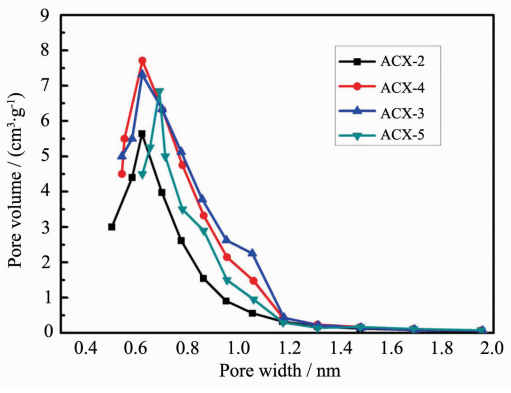

Fig.9　pore size distributions for KOH-activated samples

3　Conclusions

High-specific-surface area porous carbon xerogels were prepared by a lysine-catalyzed method and subsequent KOH activation process. The hydrogen storage properties of the porous carbon xerogels investigated at 298 K and 77 K show that the sample ACX-5 with highest surface area (2 204 $m^2 \cdot g^{-1}$) and larger micropore volume (0.6 $cm^3 \cdot g^{-1}$) exhibits the largest hydrogen capacity of 4.3wt% at 77 K and under 1.1 MPa hydrogen pressure. The hydrogen storage capacity of porous adsorbent is a function of surface area, and micropore volume as well. Furthermore, the narrow microporosity makes contribution to the H_2 storage capacity of carbon xerogels through simple physical adsorption.

References:

[1] Schlapbach L, Züttel A. *Nature*, **2001**,**414**:353-358

[2] Yang Z, Xia Y, Mokaya R. *J. Am. Chem. Soc.*, **2007**,**129**: 1673-1679

[3] Pacula A, Mokaya R. *J. Phys. Chem. C*, **2008**,**112**(7):2764-2769

[4] Xu W C, Takahashi K, Matsuo Y, et al. *Int. J. Hydrogen Energy*, **2007**,**32**(13):2504-2512

[5] Kabbour H, Baumann T F, Satcher Jr J H, et al. *Chem. Mater.*, **2006**,**18**:6085-6087

[6] Tian H Y, Buckley C E, Wang S B, et al. *Carbon*, **2009**,**47**: 2112-2142

[7] Zubizarreta L, Menéndez J A, Job N, et al. *Carbon*, **2010**, **48**:2722-2733

[8] Tian H Y, Buckley C E, Paskevicius M, et al. *Int. J. Hydrogen Energy*, **2011**,**36**:10855-10860

[9] Pekala R W. *J. Mater. Sci.*, **1989**,**24**:3221-3227

[10]Pekala R W, Alviso C T, Kong F M, et al. *J. Non-Cryst. Solids*, **1992**,**145**:90-98

[11]Pekala R W. *US Patent*, 873218. 1989-04.

[12]Pekala R W, Schaefer D W. *Macromolecules*, **1993**,**26**:5887-

5893

[13]Mulik S, Sotiriou-Leventis C, Leventis N. *Chem. Mater.*, **2007**, **19**:6138-6144

[14] Hao G P, Li W C, Qian D, et al. *Adv. Mater.*, **2010**,**22**:853-857

[15]Brunauer S, Emmett P H, Teller E. *J. Am. Chem. Soc.*, **1938**,**60**:309-319

[16]Figueroa-Torres M Z, Robau-Sanchez A, de la Torre-Saenz L, et al. *Micropor. Mesopor. Mater.*, **2007**,**98**:89-93

[17]Lozano-Castello D, Calo J M, Cazorla-Amoros D, et al. *Carbon*, **2007**,**45**:2529-2536.

[18]Ehrburger P, Addoun A, Addoun F, et al. *Fuel*, **1986**,**65**: 1447-1449

[19]Brunauer S, Emmett P H, Teller E. *J. Am. Chem. Soc*, **1938**, **60**:309-319

[20]Gregg S J, Sing K S W. *Adsorption, Surface Area and Porosity*. 2*nd Ed*, London: Academic Press, **1982**:56

[21]Wang H L, Gao Q M, Hu J. *J. Am. Chem. Soc.*, **2009**,**131**: 7016-7022

[22]Hiroki A, Tomokazu T, Ikumi T. *Int. J. Hydrogen Energy*, **2011**,**36**:580-585

[23]Armandi M, Bonelli B, Geobaldo F, et al. *Micropor Mesopor Mater.*, **2010**,**132**:414-420

[24]Zubizarreta L, Arenillas A, Pis J. *J. Int. J. Hydrogen Energy*, **2009**,**34**:4575-4581

[25]de la Casa-Lillo MA, Lamari-Darkrim F, Cazorla-Amoros D, et al. *J. Phys. Chem. B*, **2002**,**106**:10930-10934

[26]Gadiou R, Texier-Mandoki N, Piquero T, et al. *Adsorption*, **2005**,**11**:823-827

[27]Rezpka M, Lamp P, de la Casa-Lillo M A. *J. Phys. Chem. B*, **1998**,**102**:10894-10898

[28]Zubizarreta L, Gomez E I, Arenillas A, et al. *Adsorption*, **2008**,**14**:557-566

[29]Jordá-Beneyto M, Suárez-Garía F, Lozano-Castelló D, et al. *Carbon*, **2007**,**45**:293-303